Remote Sensing of Environment 170 (2015) 90–101

Contents lists available at ScienceDirect

Remote Sensing of Environment

journal homepage: www.elsevier.com/locate/rse

Performance of Landsat 8 Operational Land Imager for mapping ice sheet velocity

Seongsu Jeong *, Ian M. Howat

School of Earth Sciences, The Ohio State University, Columbus, OH 43210, USA

ARTICLE INFO

Article history:
Received 2 April 2015
Received in revised form 12 August 2015
Accepted 22 August 2015
Available online xxxx

Keywords:
Landsat 8
OLI
LDCM underfly
Glacier flow
Feature tracking

ABSTRACT

Landsat imagery has long been used to measure glacier and ice sheet surface velocity, and this application has increased with increased length and accessibility of the archive. The radiometric characteristics of Landsat sensors, however, have limited these measurements generally to only fast-flowing glaciers with high levels of surface texture and imagery with high sun angles and cloud-free conditions, preventing wide-area velocity mapping at the scale achievable with synthetic aperture radar (SAR). The Operational Land Imager (OLI) aboard the newly launched Landsat 8 features substantially improves radiometric performance compared to preceding sensors: enhancing performance of automated Repeat-Image Feature Tracking (RIFT) for mapping ice flow speed. In order to assess this improvement, we conduct a comparative study of OLI and the Landsat 7 Enhanced Thematic Mapper Plus (ETM+) performance for measuring glacier velocity in a range of surface and atmospheric conditions. To isolate the effects of radiometric quantization and noise level, we construct a model for simulating ETM+ imagery from OLI and compare RIFT results derived from each. We find that a nonlinearity in the relationship between ETM+ and OLI radiances at higher brightness levels results in a particularly large improvement in RIFT performance over the low-textured interior of the ice sheets, as well as improved performance in adverse conditions such as low sun-angles and thin clouds. Additionally, the reduced noise level in OLI imagery results in fewer spurious motion vectors and improved RIFT performance in all conditions and surfaces. We conclude that OLI imagery should enable large-area ice sheet and glacier mapping so that its coverage is comparable to SAR, with a remaining limitation being image geolocation.

1. Introduction

The accessibility, long historical archive, frequent repeat cycle and high spatial resolution of Landsat imagery make them an excellent resource for Earth surface change detection over timescales of weeks to decades. Landsat has been used to observe glacier and ice sheet surface motion, through the use of automated Repeat Image Feature Tracking (RIFT), for over two decades (e.g. Bindschadler & Scambos, 1991; Scambos & Bindschadler, 1993). This application has expanded over the past few years following the opening of access to the USGS Landsat archive, and Landsat is now a primary tool for monitoring ice sheet change (e.g. Enderlin et al., 2014). The utility of Landsat, and other optical-band imagery, for measuring ice flow, however, has been generally restricted to cloud free, daytime imagery over areas of high surface texture. These conditions are required to provide enough spatial variability in pixel brightness to enable successful cross-correlation-based matching of features between images. This limitation is largely dependent on the radiometric precision of the imagery. Increasing the precision tends to decrease the ambiguity of the cross-correlation maxima, improving match success. The 8 bit precision of Landsat radiometers through the Landsat 7 Enhanced Thematic Mapper Plus (ETM+) tends to be inadequate for tracking features over snow-covered terrain and in imagery with low illumination levels and/or with cloud or fog cover; conditions especially common at high latitudes. The Operational Land Imager (OLI) sensor aboard Landsat 8, launched in February 2013, provides imagery with 12-bit precision, a 16-fold increase over ETM+ and its predecessors. A study by Morfitt et al. (2015) positively identified that the radiometric performance such as signal-to-noise ratio (SNR) and dynamic range of OLI outperforms that of ETM+. We would therefore expect the OLI to have improved performance in feature tracking over low contrast surfaces compared to previous Landsat sensors. Here we assess this improvement.

Comparison of OLI and ETM+ performance is complicated by differences in optical band widths. The relative spectral response curves and band indices for these sensors are illustrated in Fig. 1. RIFT is most often applied to panchromatic band (number 8 for both sensors) imagery due to its higher (15 m) spatial resolution. The OLI panchromatic band spans approximately half the spectral range of the ETM+ instrument, with a resulting lower wavelength peak in response. While this narrower bandwidth is expected to increase the contrast between vegetated

* Corresponding author.
E-mail address: jeong.134@osu.edu (S. Jeong).

http://dx.doi.org/10.1016/j.rse.2015.08.023
0034-4257/

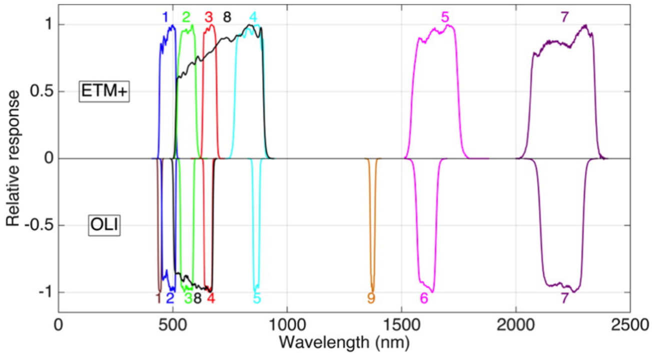

Fig. 1. Relative response curves for ETM+ (top, increasing y-axis) and OLI (bottom, decreasing y-axis) in visible and near/mid infrared range. The band designations of each sensor are as labeled on the curves.

and non-vegetated surfaces (Irons, Dwyer, & Barsi, 2012), it is unclear how this difference will impact RIFT performance over ice and snow.

A further complication in comparing sensor performance stems from the Scan Line Corrector (SLC) failure on the ETM+ in May 2003. Following SLC failure, all imagery contains void stripes, resulting in approximately 30% data loss. While the SLC failure did not impact radiometric performance (Markham et al., 2005), the presence of void stripes makes RIFT more challenging, requiring specialized processing schemes (Ahn & Howat, 2011; Warner & Roberts, 2013).

Here we compare the performance of ETM+ and OLI for RIFT of glacier flow speeds in order to assess how the increase in radiometric precision and signal-to-noise ratio impacts the quality of cross-correlation-based feature tracking. The intent is that improved understanding of the sensitivity of results to these differences will guide future sensor development and applications for change detection.

2. Method and data

Any comparative assessment of ETM+ and OLI characteristics or performance is best achieved using coincident imagery in order to ensure consistent illumination, atmospheric and ground conditions. For this purpose, ETM+ and OLI were flown in tandem mode between 29 and 30 March 2013, resulting in image acquisitions approximately 3 to 7 min apart. This tandem acquisition enables comprehensive cross validation and calibration of ETM+ and OLI radiance measurements (e.g. Mishra et al., 2014). RIFT of glacier motion using Landsat, however, requires a longer temporal separation between repeats than obtainable from the tandem mode dataset and substantial changes in environmental conditions can occur during the eight day lag between Landsat 7 and 8 passes. Thus we adopt an approach in which we compare ice flow velocity results using OLI and simulated ETM+ images. The simulated ETM+ images are created from OLI images using an ETM+/OLI radiance conversion obtained from analysis of tandem mode imagery. By using simulated imagery, we can isolate the combined effects of radiometric precision and signal to noise ratio on RIFT-derived results while ensuring equivalent illumination and environmental conditions and eliminating the influence of data gaps due to SLC failure.

2.1. OLI/ETM+ conversion and simulation

We derive a method for converting OLI quantized and calibrated digital numbers (DN) to their ETM+ equivalent using their cross relationship in the measured at-sensor radiance as observed during the 29–30 March 2013 tandem mission. Flood (2014) performed cross comparison of reflectance of each corresponding bands of ETM+ and OLI and used linear regression to estimate ETM+ reflectance from that of OLI in order to estimate biases from the normalized difference vegetation index (NDVI). In that study, the tandem underflight pair was not available due to cloud cover. Moreover, linear regression would not capture possible non-linear camera response (e.g. Dierks, 2004) in the OLI/ETM+ relationship, especially for bright pictures like snow cover.

We utilize 11 near-coincident pairs of OLI and ETM+ images obtained during the tandem mission over the Greenland Ice Sheet (Fig. 2). Coregistration errors between image pairs are determined from normalized cross correlation-based image matching (e.g. Scambos, Dutkiewicz, Wilson, & Bindschadler, 1992) of image corners detected using the method of Shi and Tomasi (1994). The images and the coregistration error statistics are listed in Table 1.

Each panchromatic image pair is converted from DN to radiance using the conversion parameters in the metadata. The overlapping area of each image pair was regridded to the same map coordinate system using bilinear interpolation, excluding void pixels. As the pixels near both ends of the swath of ETM+ are already contaminated by the void values, they were also excluded. A Gaussian filter (21×21 pixels of kernel size with $\sigma^2 = 15$) was applied to mitigate effects of noise.

Due to the non-linearity in the relationship between OLI and ETM+ radiance we do not use linear regression to derive a conversion model. Instead we construct a Lookup Table (LUT) for each tandem pair by calculating mean and number of OLI samples corresponding to ETM+ spatial bins that are equally spaced. Standard deviations of samples in each bin were also calculated to estimate the uncertainty. The mean values of each pair were weight-summed by the number of samples per bin to build a global LUT. The uncertainty of the global LUT was calculated based on that of the local curves and their weight. The mean bias in the LUT result for the eleven pairs is -0.17 and the standard deviation is 11.96 W/(m^2 srμm). These are equivalent to -0.17 and 12.26 in DN of ETM+ in low-gain mode. Considering that this bias is less than quarter of the DN quantization, and that the standard deviation is mainly due to image noise and misalignment, we observe no significant error in the LUT-based conversion.

Another difference in radiometric performance is the amount of sensor noise. Noise is considered as the standard deviation of observed radiance from a target with known constant irradiance. Scaramuzza, Markham, Barsi, and Kaita (2004) and Morfitt et al. (2015) modeled the radiance-dependent noise equivalent change in radiance of certain wavelength λ ($NE\Delta L(R_\lambda)$) as:

$$NE\Delta L(R_\lambda) = \sqrt{a + bR_\lambda} \tag{1}$$

where a and b are coefficients with different values for each ETM+ and OLI band. The noise is also affected by image smoothing from interpolation during reprojection and increased by quantization to 8-bit DN image. Including these effects into the noise model gives:

$$\nu_T(R_\lambda) = \sqrt{m \cdot NE\Delta L(R_\lambda)^2 + q^2} \tag{2}$$

where m is a factor for resampling noise scaling, 0.81 for bicubic convolution, and q is 8-bit quantization noise which is 0.281 W/(m^2 srμm) for panchromatic band of ETM+ in low gain (Scaramuzza et al., 2004).

The increase in NEΔL with the square root of radiance in Eq. (1) suggests that fluctuations in the number of detected photons, which follow a Poisson distribution, are the primary sources of noise. However, due to the large of number of photons detected per sample, and the contribution of other error sources, the noise is typically considered to follow a Gaussian distribution (e.g. Liu, Szeliski, Kang, Zitnick, & Freeman, 2008; European Machine Vision Association, 2010; Hasinoff, 2014). Thus, the measured radiance was assumed to follow a normal distribution with mean of $\mu_{R\lambda}$ and variance of $\nu(R_\lambda)^2$, thereby its mean value becomes the "measured" radiance and dispersion becomes the noise. In the noise simulation, q in Eq. (2) was set to zero because the ETM+ simulation already incorporates the effect of quantization.